

Synthesis and Characterization of New Metal–Metal Bonded Heptabromo Porphyrin

Shigeru Takagi,* Hiroyuki Furuta, Toshitaka Yagi, and Hiroyuki Yamada

Department of Environmental Technology and Urban Planning, Graduate School of Engineering,
Nagoya Institute of Technology, Gokiso-cho, Showa-ku, Nagoya 466-8555

Received April 6, 2004; E-mail: takagi.shigeru@nitech.ac.jp

A new metal–metal bonded porphyrin [(hbtbpbp)In–Mn(CO)₅], where hbtbpbp is the dianion of 2,3,7,8,12,13,17-heptabromo-5,10,15,20-tetrakis(3,5-di-*t*-butylphenyl)porphyrin, has been synthesized. In our attempt to synthesize the indium complex of octabromo porphyrin using the DMF method, we found that Br atom loss occurred in the process of metal insertion. When having synthesized the metal–metal bonded porphyrin by using a mixture of (heptabromoporphyrinato)indium and (octabromoporphyrinato)indium as the starting material, only heptabromo M–M bonded porphyrin was obtained. A large ring deformation of octabromo porphyrin disturbed the formation of the M–M bond. This heptabromo M–M porphyrin has shown high stability against electroreduction or photo-irradiation.

There has been increasing interest in the study of perhalogenated metalloporphyrin¹ as a catalyst for mono-oxygenation. Halogenations of pyrroles β -positions have been shown to confer on the efficient catalytic epoxidation and hydroxylation reactions of organic substrates. It has been shown that the substitution of electron-withdrawing groups at the pyrrole β -positions causes anodic shifts in the ring oxidation and reduction potentials of the porphyrin and an S₄ distortion of the porphyrin to a saddle shape. It was expected that the perhalogenated porphyrin would indicate attractive possibilities in fields other than catalysis. We have synthesized some metal–metal bonded indium porphyrin complexes, [(por)In–ML], where por denotes the dianion of the porphyrin ligand, and ML is a metal carbonyl moiety. We also studied the influence of the steric environment and of the electronic nature of the porphyrin ligand against a metal–metal bond.² We considered that the halogenations at the β -positions brought about a drastic change in the metal–metal bond properties. In our attempt to synthesize an indium complex of octabromo porphyrin, we found that a bromine atom displacement occurred during the metal-insertion process. Here, we report on the synthesis and properties of heptabromo porphyrin complex having a metal–metal bond, [(hbtbpbp)In–Mn(CO)₅] (Fig. 1), and a Br loss phenomenon in the indium insertion process of the octabromo porphyrin.

Experimental

Octabromoporphyrin (obtbppH₂). Perbromination of the porphyrin ligand was carried out by a modified literature method. A 100 cm³ portion of a bromine solution (4.67 g, 8.12 mmol in chloroform) was slowly added to a chloroform solution of 5,10,15,20-tetrakis(3,5-di-*t*-butylphenyl)porphyrinato copper(II), [(tbpp)Cu], (1.025 g, 0.91 mmol in 300 cm³); the resulting mixture was stirred for 4 h at room temperature. The solution color gradually changed from red to deep orange. Then, pyridine (3.7 cm³ in 100 cm³ chloroform) was added to the porphyrin solution.

After additional stirring for 15 h at room temperature, a water solution of Na₂S₂O₅ (80 g in 300 cm³) was added. The organic layer was separated, and [(obtbpp)Cu] was purified using alumina column chromatography (Merck Aluminum oxide 90, CHCl₃). Yield: 0.841 g (0.48 mmol, 53%).

After 30 cm³ of 70% perchloric acid was added to a chloroform solution of [(obtbpp)Cu] (0.84 g, 0.48 mmol, in 100 cm³), the mixture was stirred for 1 h at room temperature. The organic layer was separated and washed with an aqueous Na₂CO₃ solution. The resulting crude material was purified by alumina column chromatography. Yield: 0.627 g (0.37 mmol, 77%). Anal. Found: C, 52.98; H, 4.98; N, 3.04%. Calcd for C₇₆H₈₆N₄Br₈·H₂O: C, 53.29; H, 5.18; N, 3.27%. ¹H NMR (CDCl₃) δ 1.56 (72H, s, *t*-butyl), 7.82 (4H, s, *p*-phenyl), 8.08 (8H, s, *o*-phenyl). UV–vis (CHCl₃) λ /nm: 472, 573, 632, 746.

Indium Insertion. An indium complex of octabromoporphyrin was prepared by the DMF method. InCl₃·4H₂O (0.51 g) and obtbppH₂ (0.50 g, 0.30 mmol) were added to boiling dimethylformamide (180 cm³) and refluxed for 2 h. After cooling to room temperature, 200 cm³ of water was added. The red-purple precipitate was filtered and purified by alumina column chromatography (CHCl₃). The eluant was shaken with 30% hydrochloric acid, and the solvent was removed in vacuo. Yield, 0.44 g. UV–vis (CHCl₃) λ /nm: 471, 606, 665 nm.

Synthesis of M–M Bonded Porphyrin. A THF solution of [Mn₂(CO)₁₀] (34 mg, 0.087 mmol in 70 mL of THF) was stirred over 1% Na–Hg (68 g) for 2 h at room temperature. The resulting grayish-green supernatant was added to a 40 cm³ THF solution of brominated porphyrin (98 mg).³ After additional stirring at room temperature for 24 h, THF was distilled off at reduced pressure. The thus-obtained crude material was purified by silica-gel (Wako gel C-200) column chromatography using benzene as an eluent. Yield, 20 mg. Anal. Found: C, 50.31; H, 4.82; N, 2.92%. Calcd for C₇₇H₈₅N₄O₅Br₇InMn·H₂O: C, 50.10; H, 4.52; N, 2.89%. ¹H NMR (CDCl₃) δ 1.54 (72H, s, *t*-butyl), 7.78, 7.82, 8.20 (12H, m, phenyl), 8.80 (1H, s, pyrrole- β (H)). UV–vis (CHCl₃) λ /nm: 414, 485, 575, 620, 680.

Instrumentation and Methods. The conditions for electro-

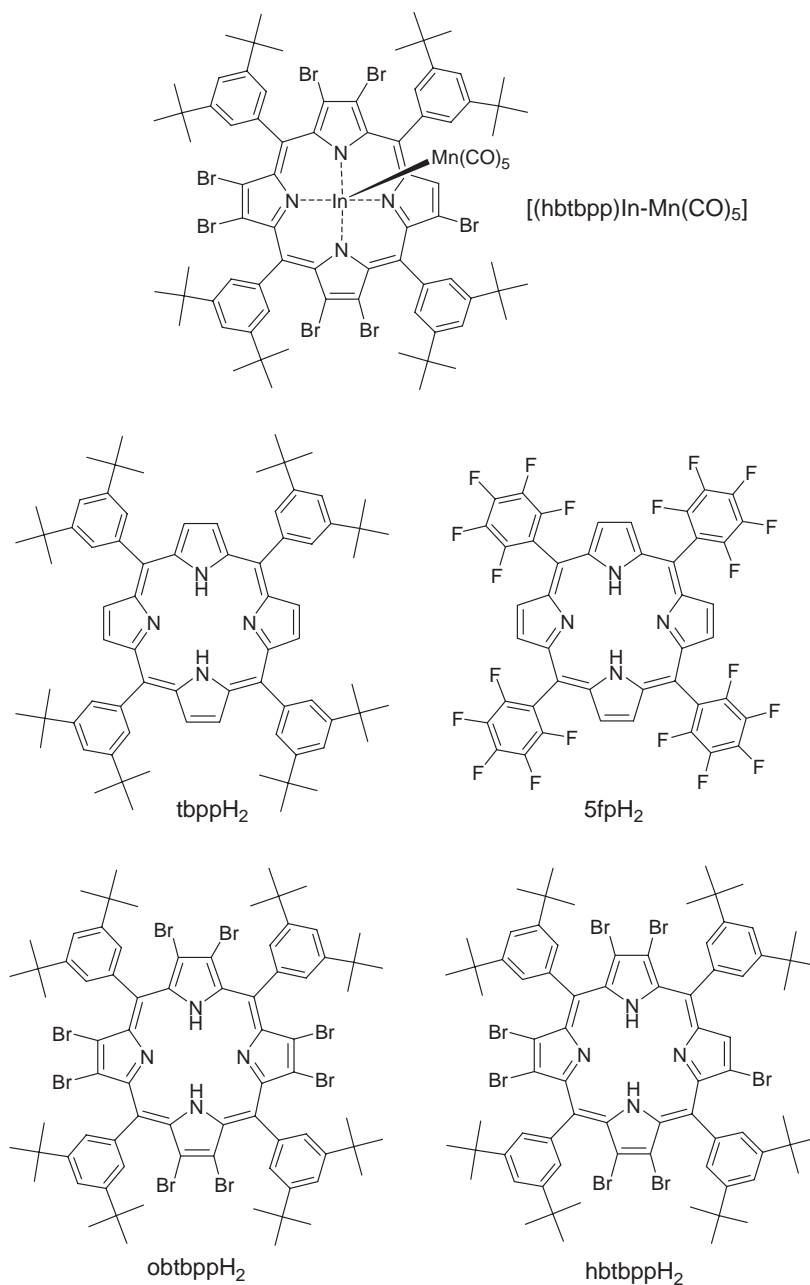


Fig. 1. Structure of 2,3,7,8,12,13,17-heptabromo-5,10,15,20-tetrakis(3,5-di-*t*-butylphenyl)porphyrinato indium(III) (pentacarbonylmanganese) $[(\text{hbtbpp})\text{In}-\text{Mn}(\text{CO})_5]$, 5,10,15,20-tetrakis(3,5-di-*t*-butylphenyl)porphyrin (tbppH_2), 5,10,15,20-tetrakis(pentafluorophenyl)porphyrin (5fpH_2), 2,3,7,8,12,13,17,18-octabromo-5,10,15,20-tetrakis(3,5-di-*t*-butylphenyl)porphyrin (obtbppH_2), and 2,3,7,8,12,13,17-heptabromo-5,10,15,20-tetrakis(3,5-di-*t*-butylphenyl)porphyrin (hbtbppH_2).

chemical measurements were as follows. The working electrode was a Pt plate, and the counter electrode was a Pt coil. We used Ag/Ag^+ (0.01 M AgNO_3 in CH_3CN) as a reference electrode. All measurements were carried out at 296 K. Approximately a 10^{-3} M solution for each sample was prepared in CH_2Cl_2 , which contained 0.1 M tetrabutylammonium perchlorate as a supporting electrolyte. All of the manipulations were carried out under an argon atmosphere. NMR spectra were measured with a Bruker AVANCE200 spectrometer in the Fourier-transform mode. The IR spectra were recorded on a JASCO Valor-III FT-IR spectrometer. UV-vis spectra were measured using a JASCO V-570 spectrometer.

Results and Discussion

Table 1 lists the λ_{max} values of porphyrins. From a study on the bromination of tppH_2 derivatives, Callot pointed out that each bromine substitution at the pyrrole position contributed to a shift of 6 nm to the red region with respect to the bands observed for tppH_2 .⁴ In obtbppH_2 porphyrin, the red-shift value of the Soret band from tbppH_2 is 46 nm, which almost corresponds to the result of octabromo tppH_2 .

In the ^1H NMR spectrum of obtbppH_2 , the signal of pyrrole β -H disappeared completely. After an indium insertion reaction, a weak pyrrole β -H signal ($\delta = 8.80$, s) was observed

Table 1. UV-Vis Absorption Maxima of Porphyrins in C₆H₆ Solution

Porphyrins	λ_{\max}/nm	
	Soret	Q band
tbppH ₂	425	520, 558, 595, 653
obtbpH ₂	472	573, 632, 746
In(tbpp)Cl	432	524, 562, 602
[In(obtbp)Cl]	471	606, 665
[(tbpp)In-Mn(CO) ₅]	388, 459	548, 591, 639
[(hbtbp)In-Mn(CO) ₅]	414, 485	575, 620, 680

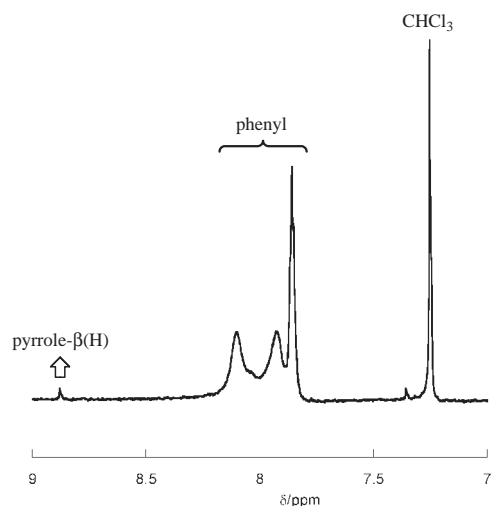


Fig. 2. Aromatic region of the ¹H NMR spectrum of the indium complex after 2 h reaction with InCl₃. A weak pyrrole β-H signal (δ = 8.80, s) has been observed. Spectrum is recorded in CDCl₃ (200 MHz) at 298 K.

(Fig. 2). When only obtbpH₂ was refluxed in DMF for 4 h, a NMR spectral change was not observed. It was confirmed that the obtained indium complex was a mixture of octabromoporphyrin [In(obtbp)Cl] and heptabromoporphyrin [In(hbtbp)Cl] by elemental analysis.⁵ An attempt to separate the [In(obtbp)Cl] from the mixture was unsuccessful by a column-chromatographic technique; we obtained [In(obtbp)Cl] by recrystallization from CH₂Cl₂/hexane.⁶ We were not able to isolate the [In(hbtbp)Cl] with sufficient purity by column chromatography or recrystallization.

D'Souza et al. have reported that the electrochemical reduction of [Co(Br_xtp)] caused a stepwise loss of Br.⁷ Such a reaction has not been reported in other metalloporphyrin systems so far. To clarify the behavior of Br loss in the process of indium insertion, the relation between the reaction time and the distribution of products was examined. The ratio of [In(obtbp)Cl] and [In(hbtbp)Cl] was estimated from the integral values of pyrrole β-H and the phenyl-H. Bromine atom loss was hardly observed when the reaction time was within 1 h, though the total yield was only about 10%. When reacting for 2 h or more, the overall yield of indium insertion reached 70–80% and [In(hbtbp)Cl] became the dominant species. Though the reaction time was lengthened to examine whether the second Br loss occurred, it was not able to make a confirmation because of porphyrin ring decomposition over 24 h.

The porphyrin ring deformation of [In(obtbp)Cl] is larger than that of [In(hbtbp)Cl]; [In(obtbp)Cl] might be changed into the more stable [In(hbtbp)Cl] as the reaction time becomes long. We speculate Br loss mechanism is as follows: The formaldehyde caused by the decomposition of DMF has reduced the In³⁺ to In⁺ and this In⁺ causes the Br displacement from the porphyrin ring.⁸

Our entire attempt to synthesize [(obtbp)In-Mn(CO)₅] using [In(obtbp)Cl] was unsuccessful; we used a mixture of [In(hbtbp)Cl] and [In(obtbp)Cl] as the starting material, and obtained a green compound. From an elemental analysis and the ¹H NMR spectrum, it was confirmed that the obtained green compound was [(hbtbp)In-Mn(CO)₅]. A large steric hindrance of obtbp disturbed the formation of a metal-metal bond. The red-shift value of the Soret band between [(hbtbp)In-Mn(CO)₅] and [(tbpp)In-Mn(CO)₅] was 26 nm; this red shift clearly shows a change in the electronic nature of the porphyrin unit, though this value is small compared with the shift in freebase. Carbonyl stretching frequencies in the IR measurements are considerably sensitive to the electronic nature of the porphyrin unit. We have already found that higher frequency shifts are in inverse proportion to the σ-donor ability of the porphyrin unit based on a study of (por)In-ML complexes, where por = oep, tpp, tbpp, and 5fp. The carbonyl stretching frequency of [(hbtbp)In-Mn(CO)₅] (2083, 1989 cm⁻¹, benzene solution) is higher than that of [(tbpp)In-Mn(CO)₅] (2079, 1972 cm⁻¹, benzene solution). This result corresponds well with the lower σ-donor ability of hbtbp.

Kadish et al. reported that a nonlinear relationship was observed between *E*_{1/2} for the first oxidation of [M(Br_xtp)] and the number of Br groups on the compound.⁹ On the contrary, the first reduction of [M(Br_xtp)] was linearly related to the number of Br. Kadish suggested that not only inductive effects of the Br governed the oxidation potentials, but also by saddle deformations of the porphyrin ring, and that the ring deformation should have a minimum effect on the reduction potentials. To investigate the effects of halogen substitutions on the pyrrole β-positions, we examined the redox properties of [(tbpp)In-Mn(CO)₅] and [(hbtbp)In-Mn(CO)₅] using cyclic voltammetry. For a comparison, a CV measurement of [(5fp)In-Mn(CO)₅] was made; 5fp showed no ring deformation, and only the inductive effect of F worked concerning the redox properties. Typical cyclic voltammograms are illustrated in Figs. 3 and 4. The redox potentials of three M-M bonded porphyrins are listed in Table 2. The oxidation step (porphyrin ring oxidation to a π-cation radical) is completely irreversible in each porphyrin. Oxidized In-Mn bonded porphyrin undergoes a rapid cleavage of the In-Mn bond to generate [(P)In]⁺ and Mn(CO)₅ radical in solution.¹⁰ The order of the oxidation potential is [(tbpp)In-Mn(CO)₅] < [(hbtbp)In-Mn(CO)₅] < [(5fp)In-Mn(CO)₅]. Though the influence of the inductive effect of halogen atoms is predominant in the oxidation potential, this influence has been somewhat counterbalanced in [(hbtbp)In-Mn(CO)₅] due to saddle deformation. Each M-M bonded porphyrin undergoes two reductions in the potential range of CH₂Cl₂. The values of *E*_{1/2} show that the influence of the inductive effect of halogen atoms is almost the same between in [(hbtbp)In-Mn(CO)₅] and [(5fp)In-Mn(CO)₅]. The first reduction step (porphyrin ring reduction

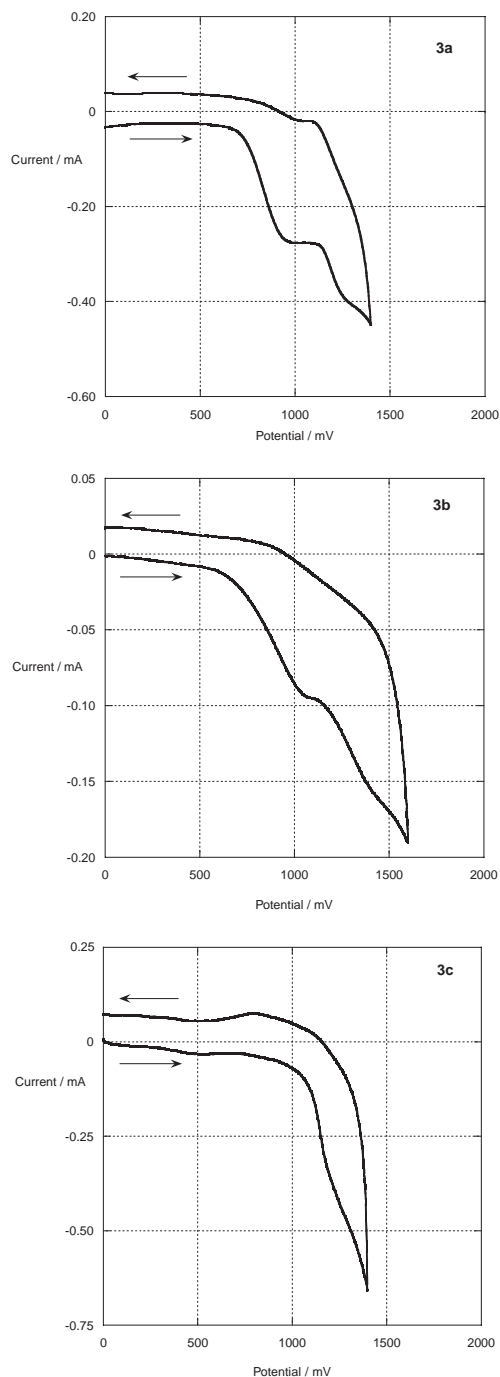


Fig. 3. Cyclic voltammograms (oxidative scan) of M–M bonded porphyrins, (a) [(tbpp)In–Mn(CO)₅], (b) [(hbtbtp)In–Mn(CO)₅], and (c) [(5fp)In–Mn(CO)₅] in CH₂Cl₂ at room temperature. For measurement conditions, see Table 2.

to an anion radical) is nearly reversible in each porphyrin, and the reversibility of [(tbpp)In–Mn(CO)₅] is inferior to those of the other two porphyrins. The peak current of each reduction is proportional to the square root of the scan rate, indicating a diffusion-controlled process.

The appearance of an oxidation peak at -0.43 V was observed in all three porphyrins. This peak is assigned to the oxidation of Mn(CO)_5^- . The irreversible chemical reaction cou-

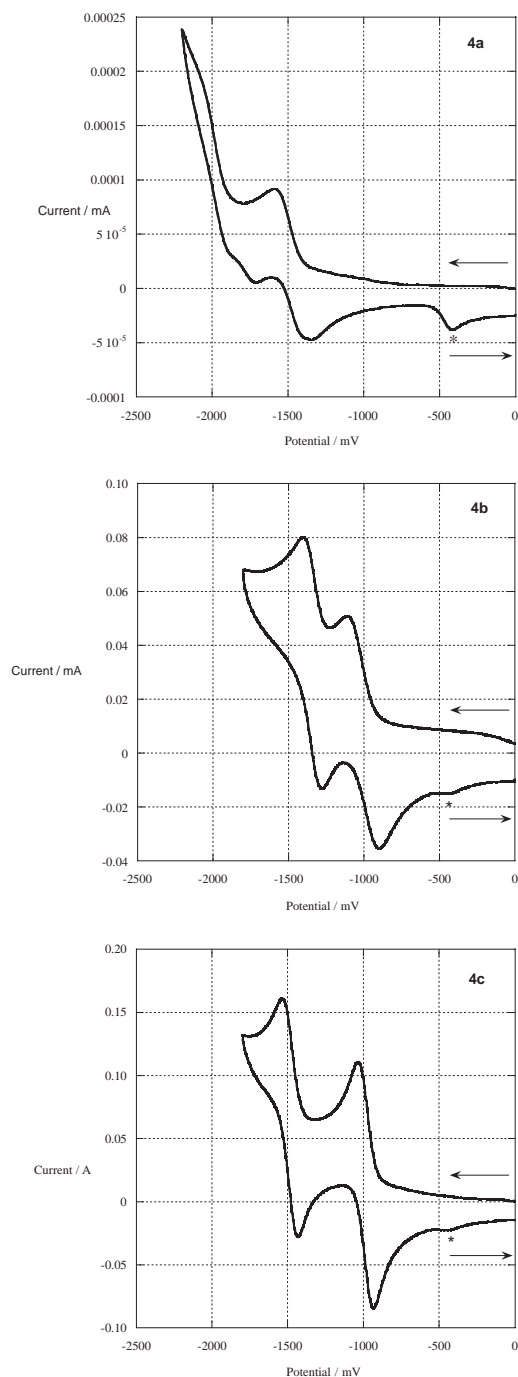


Fig. 4. Cyclic voltammograms (reductive scan) of M–M bonded porphyrins, (a) [(tbpp)In–Mn(CO)₅], (b) [(hbtbtp)In–Mn(CO)₅], and (c) [(5fp)In–Mn(CO)₅] in CH₂Cl₂ at room temperature. For measurement conditions, see Table 2. The asterisks (*) indicate the oxidation peaks of Mn(CO)_5^- .

pled to the first electroreduction step corresponds to a cleavage of the In–Mn bond.⁹ The oxidation peak of Mn(CO)_5^- is obviously large in [(tbpp)In–Mn(CO)₅] compared to [(hbtbtp)In–Mn(CO)₅] (see Figs. 4a and 4b). This result indicates that the M–M bond of [(hbtbtp)In–Mn(CO)₅] is more stable than that of [(tbpp)In–Mn(CO)₅] against electroreduction.

Table 2. Redox Potentials of the M–M Bonded Porphyrins at Ambient Temperature (CH₂Cl₂, 0.1 M TBAP; Pt Working Electrode; Ag/AgNO₃ Reference Electrode; 100 mV s^{−1} Scan Rate)

Porphyrins	E_p^{OX}/V	$E_{1/2}^{Red1}/V$	$E_{1/2}^{Red2}/V$
[(tbbp)In–Mn(CO) ₅]	+0.94 ^{a)}	−1.44	−2.01
[(hbtbtp)In–Mn(CO) ₅]	+1.06 ^{a)}	−1.00	−1.34
[(5fp)In–Mn(CO) ₅]	+1.20 ^{a)}	−0.99	−1.51

a) Redox potential values for irreversible processes.

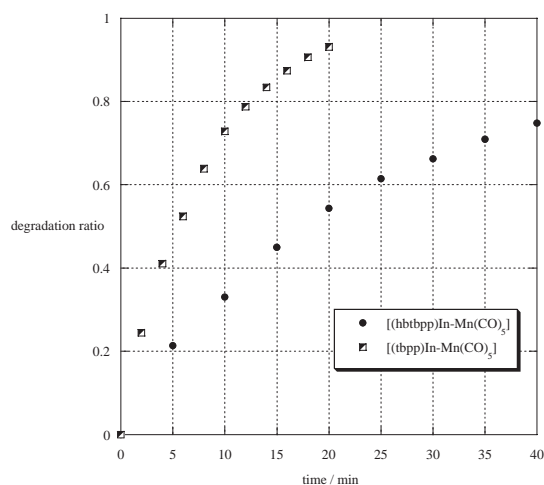


Fig. 5. Plots showing the degradation ratio ($1 - [C]/[C_0]$) of M–M bonded porphyrins with time during photo-irradiation based on the absorption spectra.

In order to examine the influence of bromine substitution on the metal–metal bond stability, we conducted a kinetic experiment of metal–metal bond degradation by light irradiation.¹¹ The color of the benzene solution changed from green to pink upon photo irradiation. After degradation of the M–M bond occurred, pink-colored (por)In–OH was formed by reacting with water contained in the solvent. The degradation ratio ($1 - [C]/[C_0]$), where the initial concentration (C_0) was 2.0×10^{-6} mol/L, of metal–metal bond porphyrin was determined by a UV–vis spectra measurement. Plots of ($1 - [C]/[C_0]$) versus time are shown in Fig. 5. The degradation rate constant of [(hbtbtp)In–Mn(CO)₅] is about 3.5-times smaller than that of [(tbbp)In–Mn(CO)₅].¹² This result and electroreduction results clearly show that the substitution of bromine at the pyrrole β -positions brings about a higher stability of the metal–metal bond. A photoinduced cleavage of the indium–carbon bond in (por)In–R resulted in the formation of a zwitterionic (por)[−](In^{III})⁺, and the magnitude of the photochemical quantum yield of the M–C bond cleavage was shown to decrease with increasing electron-withdrawing character of the porphyrin macrocycle.¹³ When thinking that the electrochemical behavior and photodissociative behavior of [(por)In–Mn(CO)₅] are similar to those of [(por)In–R], it seems reasonable to assume that the cleavage of M–M bond results from the formation of the zwitterion (por)[−](In^{III})⁺. Proposed mechanisms are shown in Fig. 6.

The increased electron donicity of tbbp with respect to that of hbtbtp stabilizes the zwitterion (por)[−](In^{III})⁺; therefore, the

(a) photo-irradiation



(b) electroreduction

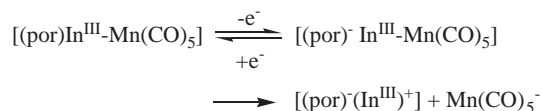


Fig. 6. Proposed mechanisms of M–M bond cleavage, (a) photo-irradiation, (b) electroreduction.

M–M bond cleavage of [(tbbp)In–Mn(CO)₅] occurs easily compared with that of [(hbtbtp)In–Mn(CO)₅]. Although it is not clear whether the saddle deformation of the porphyrin ring influences the M–M bond stability, it is likely that the electron-withdrawing property of the porphyrin ring plays a large part in the stability of the M–M bond.

We are grateful to Professor Shuki Araki (Nagoya Institute of Technology) for helpful discussions.

References

- a) H. J. Callot, *Bull. Soc. Chim.*, **7–8**, 1492 (1974). b) T. G. Traylor and S. Tsuchiya, *Inorg. Chem.*, **26**, 1338 (1987). c) P. Hoffman, G. Labat, A. Robert, and B. Meunier, *Tetrahedron Lett.*, **31**, 1991 (1990). d) P. Battioni, O. Brigaud, H. Desvaux, D. Mansui, and T. G. Traylor, *Tetrahedron Lett.*, **32**, 2893 (1991). e) P. Bryrappa and V. Krishnan, *Inorg. Chem.*, **30**, 239 (1991). f) D. Ostovic and T. C. Bruice, *Acc. Chem. Res.*, **25**, 314 (1992). g) D. Mandon, P. Ochsenbein, J. Fischer, R. Weiss, K. Jayaraj, R. N. Austin, A. Gold, P. S. White, O. Brigaud, P. Battioni, and D. Mansuy, *Inorg. Chem.*, **31**, 2044 (1992). h) F. D'Souza, A. Villard, E. V. Caemelbecke, M. Franzen, T. Boschi, P. Tagliatesta, and K. M. Kadish, *Inorg. Chem.*, **32**, 4042 (1993). i) E. R. Birnbaum, J. A. Hodge, M. W. Grinstaff, W. P. Schaefer, L. Henling, J. A. Labinger, J. B. Bercaw, and H. B. Gray, *Inorg. Chem.*, **34**, 3626 (1995). j) M. W. Grinstaff, M. G. Hill, E. R. Birnbaum, W. P. Scafer, J. A. Labinger, and H. B. Gray, *Inorg. Chem.*, **34**, 4896 (1995). k) M. Tabata, J. Nishimoto, A. Ogata, T. Kusano, and N. Nahar, *Bull. Chem. Soc. Jpn.*, **69**, 673 (1996). l) R. A. Richards, K. Hammons, M. Joe, and G. M. Minskelly, *Inorg. Chem.*, **35**, 1940 (1996). m) M. Tabata, T. Kusano, and J. Nishimoto, *Anal. Sci.*, **13**, 157 (1997).
- S. Takagi, Y. Kato, H. Furuta, S. Onaka, and T. K. Miyamoto, *J. Organomet. Chem.*, **429**, 287 (1992).
- The mixture of [In(obtbbp)Cl] and [In(hbtbtp)Cl].
- H. J. Callot and E. Schaffer, *Nouv. J. Chim.*, **4**, 311 (1980).
- Anal. Found: C, 50.34; H, 4.82; N, 2.72%. Calcd for C₇₆H₈₄N₄Br₈InCl (octabromo): C, 49.53; H, 4.59; N, 3.04% Calcd for C₇₆H₈₅N₄Br₇InCl (heptabromo): C, 51.74; H, 4.86; N, 3.18%.
- Anal. Found: C, 49.64; H, 4.68; N, 2.77%. Calcd for C₇₆H₈₄N₄Br₈InCl: C, 49.53; H, 4.59; N, 3.04%.
- F. D'Souza, A. Villard, E. Van Caemelbecke, M. Franzen, T. Boschi, P. Tagliatesta, and K. M. Kadish, *Inorg. Chem.*, **32**, 4042 (1993).
- Though indium insertion was tested with various solvents other than DMF to examine the influence of the formaldehyde, the reaction was hardly occurred.
- a) K. M. Kadish, F. D'Souza, A. Villard, M. Autret, E. V.

Caemelbecke, P. Bianco, A. Antonini, and P. Tagliatesta, *Inorg. Chem.*, **33**, 5169 (1994). b) P. Tagliatesta, J. Li, M. Autret, E. V. Caemelbecke, A. Villard, F. D'Souza, and K. M. Kadish, *Inorg. Chem.*, **35**, 5570 (1996). c) F. D'Souza, M. E. Zandler, P. Tagliatesta, A. Ou, J. Shao, E. V. Caemelbecke, and K. M. Kadish, *Inorg. Chem.*, **37**, 4567 (1998).

10 R. Guillard, P. Mitaine, C. Moïse, C. Leomte, A. Boukhris, C. Swistak, A. Tabard, D. Lacombe, J.-L. Cornillon, and K. M.

Kadish, *Inorg. Chem.*, **26**, 2467 (1987).

11 Light irradiation was carried out by using 500 W tungsten lamp.

12 The value of degradation rate constant k was estimated by thinking simple first-order reaction.

13 K. M. Kadish, G. B. Maiya, and Q. Y. Xu, *Inorg. Chem.*, **28**, 2518 (1989).